Identifying the Effect of Non-Ideal Mixing on a Pre-Denitrification Activated Sludge System Performance through Model-Based Simulations

Malek Hajaya

Civil Engineering Department, Tafila Technical University, Tafila 66110, Jordan

Effectiveness of a pre-denitrification activated sludge treatment system is governed by the kinetics of the biological reactions, and the hydrodynamic mixing behavior in the reactors. Achieving good mixing conditions within a reactor not only enhances the transfer of reactants but also ensures homogeneous environmental conditions throughout the vessel when required, allowing for an effective usage of the reactor's total volume, leading to optimized, low-cost operation. In this work, a pre-denitrification activated sludge system performance with regards to the biological treatment of organic carbon and nitrogen was investigated, under two scenarios for non-ideal mixing in the anoxic reactor. The system performance is simulated based upon the Activated Sludge Model 1 model's biological reactions, and combining two non-ideal mixing two-parameter models: CSTR with bypass and dead volume, and two CSTRs with exchange. Performance discrepancies were then identified in the presence of non-ideal mixing. The system's performance was found to be more susceptible to the presence of a dead volume/bypass scenario compared to the two CSTRs with material exchange scenario. Under non-ideal mixing conditions, effluent concentrations of Total Kjeldahl Nitrogen, organic carbon increased marginally, while effluent concentration of nitrate increased significantly. Similarly, the waste stream concentrations of Total Kjeldahl Nitrogen and organic carbon increased significantly as a result of an increase in the concentration of the heterotrophic biomass. The outcome of this study provides an insight when troubleshooting the operation of pre-denitrification activated sludge systems for non-ideal mixing conditions.

Keywords: Non-ideal mixing, Activated sludge, Dead volume, Bypass, Material exchange

Introduction

Activated Sludge (AS) systems are among the most widely employed biological treatment processes in wastewater treatment plants(Rittmann and McCarty, 2001). AS systems are engineered processes, designed and operated to sustain and facilitate the growth of different microorganisms. These microorganisms in their part treat wastewaters biologically by incorporating/removing the pollutants in their different metabolic and growth associated processes. Those pollutants are mainly comprised of dissolved and particulate organic carbon and nitrogen-containing compounds. The main biological processes leading to wastewater treatment taking place in AS systems, and the associated microorganisms responsible for them are organic carbon mineralization under aerobic and anoxic conditions by facultative heterotrophic bacteria, ammonia (NH_3) oxidization under aerobic conditions to nitrate (NO_3^{-1}) by autotrophic nitrifying bacteria, and nitrate reduction under anoxic conditions to nitrogen gas (N_2) by the aforementioned facultative heterotrophic bacteria (utilized instead of oxygen in the metabolic process) (Madigan and Martinko, 2006; Tchobanoglous *et al*., 2007). Pre-denitrification is (PD) one approach for the operation of AS (Hellinga *et al*., 1999; Kim *et al*., 2009). The required environmental conditions (anoxic and aerobic) are divided between two distinctive Continuous-flow stirred-tank reactors (CSTRs), and the microorganisms (biomass) are circulated between them. **Figure 1** illustrates the process scheme. The anoxic reactor receives both fresh organic carbon and ammonia containing wastewater and a nitrate-rich, biomass containing, mixed liquor recycle from the aerobic reactor, where a portion of organic carbon is mineralized and nitrate is reduced to nitrogen gas. Anoxic reactor effluent carries the remaining untreated wastewater to the aerobic reactor, where air is supplied to sustain an elevated oxygen concentration, and enhanced mixing conditions. The remaining organic carbon is completely mineralized and ammonia is oxidized to nitrate. The settler allows for biomass to be separated from the mixed liquor, and recycled back so that the system's solids retention time is controlled independently from the system's hydraulic retention time (Tchobanoglous *et al*., 2007). Effectiveness of a PD-AS treatment system is governed by the kinetics of the biological reactions, and the hydrodynamics of mixing in the reactors. The different reactions and processes taking place in a PD-AS system were first identified and modeled by the International Water Association (IWA) Activated Sludge Model 1 (ASM1) (Henze *et al*., 2000), and since employed in a wide variety of studies (Alex *et al*., 2008; Hajaya and Pavlostathis, 2013; Ostace *et al*., 2011; Van Loosdrecht *et al*., 2015). ideal mixing conditions are commonly assumed while designing biological reactors for wastewater treatment processes (Vanrolleghem *et al*., 2003). Achieving good mixing conditions within reactors not only enhances the transfer of substrates (reactants) but also ensures homogeneous environmental conditions throughout the vessel, thereby, allowing for an effective usage of the reactor's total volume leading to optimized and low-cost operation (Badkoubi *et al*., 1998; García *et al*., 2005).

Received on January 27, 2019, accepted on April 13, 219. Correspondence concerning this article should be addressed to Malek Hajaya (E-mail address: malekhajaya@yahoo.com or mhajaya@ttu.edu.jo).ORCiD ID for Malek Hajaya: https://orcid.org/0000-0003-0110-6731

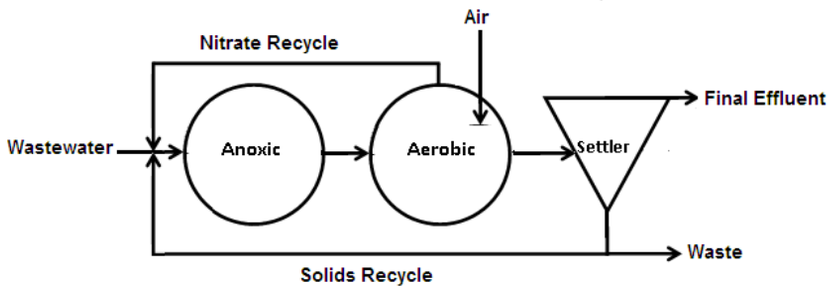

Fig. 1 Typical pre-denitrification activated sludge system including anoxic and aerobic reactors and settler

Despite the assumption of ideal mixing in biological reactors, it is likely non-ideal mixing conditions will prevail in the real situation. Kjellstrand (2006) studied the hydraulic behavior of a denitrifying activated sludge tank, located at the Rya Wastewater treatment plant (WWTP) in Göteborg Sweden, where it was found that up to 30% of the feed had notably fast hydraulic retention times, while up to 21% of the feed had notably slow hydraulic retention times compared to the nominal hydraulic retention time. This indicated the presence of feed bypass and stagnation zones in the system. Sánchez and coworkers (Sánchez *et al*., 2016) performed the hydraulic characterization for the secondary treatment system in the WWTP of San Pedro del Pinatar. They reported that only 70.5% of the system's volume was active, while the remaining 29.5% was actually a dead volume. Collivignarelli and coworkers (Collivignarelli *et al*., 2018) reported a dead volume fractions ranging from 15% to 25%, and bypass fractions ranging between 35% and 40%, while performing the experimental verification of reactor hydrodynamics for an undisclosed WWTP. Manenti and coworkers (Manenti*et al*., 2018) have identified a 5% fraction of dead volume in a pilot-scale WWTP. Non-ideal mixing occurrences in AS systems were reported for constructed, operational wastewater treatment plants, which could be brought by poor design or equipment failure. The cost of diagnosing their presence in such systems could be drastically reduced if mathematical simulations are used. The purpose of this work is to identify the possible consequences of non-ideal mixing on the biological processes performance. Such discrepancies in performance can be used in identifying the presence of non-ideal mixing behavior in the AS system reactors. In this work, a pre-denitrification activated sludge (PD-AS) unit performance with regards to the biological treatment of organic carbon and nitrogen is investigated under the conditions of non-ideal mixing in the anoxic reactor. The system performance is simulated based upon the ASM1 model's biological reactions (Henze *et al*., 2000), and combining two non-ideal mixing two-parameter models: CSTR with bypass and dead volume, and two CSTRs with exchange (Fogler, 1999). Performance discrepancies could then be identified by comparing the performance of the system under non-ideal mixing to performance of the system at ideal mixing conditions.

1. Mathematical Models

1.1 Biological reactions

The ASM1 model identified the specific processes in PD-AS to be: aerobic growth of heterotrophs, anoxic growth of heterotrophs, aerobic growth of autotrophs, decay of heterotrophs, decay of autotrophs, ammonification of soluble organic nitrogen, hydrolysis of entrapped organics, and hydrolysis of entrapped organic nitrogen (Henze *et al*., 2000). **Tables 1** detail each process mathematical model, where *S* denotes the soluble constituents' concentrations, and *X* denotes particulate constituents' concentrations, while **Table 2** lists the different variables associated with the aforementioned processes, with the kinetics of each step involved in the PD-AS system.

1.2 Ideal completely mixed reactors model

Figure 2 shows the PD-AS system. In this work, both the widely adapted COAST benchmark and BSM1 benchmark(Alex *et al*., 2008; Copp, 2002) are used for system size, albeit with some modifications. The system is designed for an average wastewater flow rate (Q) of 18400m^3/day, with≈300 mg COD/L of biodegradable organic carbon and ≈50mg N/L of nitrogen. Volumes of the anoxic and aerobic reactors are 2000 m^3 (V_1) and 4000 m^3 (V_2), respectively, with nitrate, recycle ratio (R_1) and solids recycle ratio (R_2) of 3 and 1, respectively. The waste flow rate (Q_w) is chosen for a 16-day *SRT* to be at 385m^3/day. Air is only introduced into the aerobic reactor to sustain an oxygen concentration of 2.1 ± 0.11 mg/l. The settler sub-model is not included in the system, and it is assumed that no reactions are taking place in it; instead, a particulates separation coefficient (*SE*) is assumed and used to calculate the concentration in the settler overflow (final effluent) and underflow. Particulate concentration (X) in both the settler's overflow (X_{OF}) and underflow (X_{UF}) is determined by mass balance around the settler, by using a settling efficiency (*SE*), which is assumed constant (Le Moullec *et al*., 2011) and can be defined as *SE*=Particulate mass in the underflow/ Particulate mass in the overflow:

$$X_{UF} = [SE.Q.X_2.(R_2+1)]/[R_2.Q+Q_W]\ldots \quad (1)$$
$$X_{OF} = [(1-SE).Q.X_2.(R_2+1)]/[Q+Q_W]\ldots \quad (2)$$

where X_2 is particulate concentration (mg COD/l) in the aerobic reactor.

Table 1 Biological processes taking place in the PD-AS, adapted from the ASM1 model (Henze *et al*., 2000)

Process	Model	Symbol
Aerobic growth of heterotrophs	$\mu_H \frac{S_s}{S_s+K_s}\frac{S_O}{S_O+K_{OH}}X_{BH}$	P_1
Anoxic growth of heterotrophs	$\mu_H \frac{S_s}{S_s+K_s}\frac{K_{OH}}{S_O+K_{OH}}\frac{S_{NO}}{S_{NO}+K_{NO}}\eta_G X_{BH}$	P_2
Aerobic growth of autotrophs	$\mu_A \frac{S_{NH}}{S_{NH}+K_s}\frac{S_O}{S_O+K_{OA}}X_{BA}$	P_3
Decay of heterotrophs	$b_H X_{BH}$	P_4
Decay of autotrophs	$b_A X_{BA}$	P_5
Ammonification of soluble organic nitrogen	$k_a S_{ND} X_{BH}$	P_6
Hydrolysis of entrapped organics	$k_h \frac{X_s/X_{BH}}{X_s/X_{BH}+K_X}\left[\frac{K_{OH}}{S_O+K_{OH}}+\eta_h\frac{S_{NO}}{S_{NO}+K_{NO}}\frac{K_{OH}}{S_O+K_{OH}}\right]X_{BH}$	P_7
Hydrolysis of entrapped organic nitrogen	$P_7\frac{X_{ND}}{X_S}$	P_8

Table 2 State variables in the PD-AS model and their associated rates

Variable	Definition	Rate
S_I[a]	Soluble inert organics	$r_{SI}=0$
S_S[a]	Readily biodegradable (soluble) substrate	$r_{Ss}=\frac{-1}{y_H}(P_1+P_2)+P_7$
X_I[a]	Particulate inert organics	$r_{XI}=0$
X_S[a]	Slowly biodegradable (particulate) substrate	$r_{Xs}=(1-f_P)(P_4+P_5)-P_7$
X_{BH}[a]	Active heterotrophic biomass	$r_{XBH}=P_1+P_2-P_4$
X_{BA}[a]	Active autotrophic biomass	$r_{XBA}=P_3-P_5$
X_P[a]	Non-biodegradable particulates	$r_{Xp}=f_P(P_4+P_5)$
S_O[b]	Dissolved oxygen	$r_{So}=-\frac{1-y_H}{y_H}P_1-\frac{4.57-y_A}{y_A}P_3$
S_{NO}[c]	Nitrate	$r_{SNO}=\frac{1-y_H}{2.86y_H}P_2+\frac{1}{y_A}P_3$
S_{NH}[c]	Free and ionized ammonia	$r_{SNH}=\left(-i_{XB}-\frac{1}{y_A}\right)P_3-i_{XB}(P_1+P_2)+P_6$
S_{ND}[c]	Soluble biodegradable organic nitrogen	$r_{SND}=P_8-P_6$
X_{ND}[c]	Particulate biodegradable organic N	$r_{XND}=(i_{XB}-i_{XP}f_P)(P_4+P_5)-P_8$
S_{ALK}[d]	Alkalinity	$r_{SALK}=P_7\frac{X_{ND}}{X_S}$

a: mg COD/L, mg of Chemical Oxygen Demand; b: mg O_2/ L; c: mg N/ L; d: mol/L.

Assuming ideal CSTR behavior in the anoxic and aerobic reactors, constant liquid densities and reactor volumes, and reactions taking place only in the reactors, the following equations can be used to describe the dynamic behavior of soluble (*S*) and particulate constituents:

For the anoxic reactor:

$$dS_1/dt = (Q/V_1)\left([S_i+S_2(R_1+R_2)]-[1+R_1+R_2]S_1\right)+r_{S1}\ldots \quad (3)$$
$$dX_1/dt = (Q/V_1)\left([X_i+X_2R_1+X_{UF}R_2]-[1+R_1+R_2]X_1\right)+r_{X1}\ldots \quad (4)$$

For the aerobic reactor:

$$dS_2/dt = (Q[1+R_1+R_2]/V_2)\,(S_1-S_2)+r_{S2}\ldots \quad (5)$$
$$dX_2/dt = (Q[1+R_1+R_2]/V_2)\,(X_1-X_2)+r_{X2}\ldots \quad (6)$$

Where S_1 and X_1 are the concentrations in the anoxic reactor, S and X_i are the concentrations in the feed wastewater (**Table 3**), and S_2 and X_2 are the concentrations in the aerobic reactor, respectively. X_{UF} is the particulate concentrations in the solids recycle (Equation 1), and $r_{S1\&S2}$ and $r_{X1\&X2}$ are the rates in the different reactors (Table 2). Finally for oxygen, in the aerobic reactor, the following rate is

introduced to represent the aeration rate ($r_{Air\text{-}in}$):

$$r_{Air-in} = K_L(S_O^{SAT} - S_{O2}) \quad (7)$$

where K_L is the oxygen transfer coefficient (d^{-1}) maintained at a level in the aerobic reactor to provide a constant oxygen concentration (as mentioned above)(Alex *et al*., 2008), and S_O^{SAT} is oxygen saturation concentration =8mg/L, (at 26°C and 1atm) (Rittmann and McCarty, 2001), and S_{O2} in the oxygen concentration in the aerobic reactor (mg/L).

1.3 Non-ideal mixing models

Among the PD-AS system reactors, the anoxic reactor is the most susceptible to the occurrence of non-ideal mixing. Mixing in this reactor is solely performed mechanically, compared to superior mixing conditions (minimizing non-ideal mixing) brought by the aeration process taking place in the aerobic reactor. Accordingly, the non-ideal mixing scenarios are assumed to affect the anoxic reactor in the PD-AS. Oxygen concentration and settler behavior are handled in the same matter as discussed above in the ideal CSTR based system.

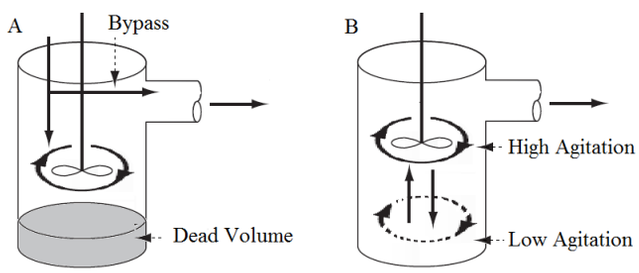

Fig. 2 Non-ideal, real mixing scenarios; A: Bypass with dead volume, and B: Rapid and slow mixing.

1.3.1 CSTR with bypass and dead volume

In this situation, poor mixing results in generating a dead zone within the reactor volume, where limited or no exchange of material is taking place between it and the remaining reactor volume. This will reduce the available volume for reactions within the reactor itself. In addition, poor mixing can allow for a portion of the feed to exit rapidly without being mixed inside the reactor, as if that portion is totally not entering the reactor, but rather bypassing it directly to the effluent (**Figure 2.A**). Previous scenarios are modeled as a combination of an ideal CSTR coupled with a dead zone. These volumes are defined as fractions of the total reactor volume (V), where α = *volume of CSTR*/V and (1-α) = *volume of dead zone*/V. On the other hand, flow rates headed for the reactor (Q) have a fraction that bypasses it while the remaining fraction enters it, where β= *bypassed flow*/Q and (1-β)= *entering flow*/Q (Fogler, 1999). The degree of nonideality depends on the values of α and β. The presence of a bypass and a dead volume in real engineered biological reactors has been previously reported (Collivignarelli *et al*., 2018; Kjellstrand, 2006; Manenti *et al*., 2018; Sánchez *et al*., 2016). In light of the previous argument, the dynamic behavior of soluble and particulate constituents in both reactors no longer behaves as described by Equations 3, 4, 5, and 6. Assuming constant values for α, β (for all streams entering), liquid densities and reactor volumes, and reactions taking place only in the reactors, the following equations can be used to describe the dynamic behavior of soluble and particulate constituents:

For the anoxic reactor:

$$dS_1/dt = (Q(1-\beta)/\alpha V_1)\,([S_i + S_2(R_1+R_2)] - [1 + R_1 + R_2]S_1) + r_{S1}\ldots \quad (8)$$

$$dX_1/dt = (Q(1-\beta)/\alpha V_1)\,([X_i + X_2R_1 + X_{UF}R_2] - [1 + R_1 + R_2]X_1) + r_{X1}\ldots \quad (9)$$

For the aerobic reactor:

$$dS_2/dt = (Q/V_2)\left((1-\beta)[1 + R_1 + R_2]S_1 + \beta[S_i + S_2(R_1+R_2)] - [1 + R_1 + R_2]S_2\right) + r_{S2}\ldots \quad (10)$$

$$dX_2/dt = (Q/V_2)\left((1-\beta)[1 + R_1 + R_2]X_1 + \beta[X_i + X_2R_1 + X_{UF}R_2] - [1 + R_1 + R_2]X_2\right) + r_{X2}\ldots \quad (11)$$

1.3.2 Two CSTRs with material exchange

This scenario depicts a situation where mixing apparatus are poorly situated within the reactor, resulting in rapid mixing in their vicinity, while the remaining region undergoes mixing, albeit at a lesser rate. This situation will influence the distribution of material within the reactor, affecting the different reactions rates due to an uneven distribution of substrates (**Figure 2.B**). In this situation, it is assumed that the anoxic reactor volume (V) is split into two fractions: a fraction that undergoes high agitation (α=highly agitated volume/V) and a fraction with low agitation ((1-α)=volume with less agitation/V). Material is exchanged between the two-volume

from the highly agitated portion (Fogler, 1999). As with the previous model, the degree of nonideality depends on the values of α and β. The two CSTR with exchange model has been previously used to describe non-ideal mixing in different biological reactors (Le Moullec *et al*., 2010; Le Moullec *et al*., 2011; Pereira *et al*., 2012). Assuming constant values for α, β (for all streams entering), liquid densities and reactor volumes, and reactions taking place only in the reactors, the following equations can be used to describe the dynamic behavior of soluble and particulate constituents:

For the anoxic reactor highly agitated fraction (concentrations are accented with 1):

$$dS^1{}_1/dt = (Q(1+R_1+R_2)/\alpha V_1)\left([S_i + S_2(R_1+R_2)/1+R_1+R_2] - S^1{}_1 + \beta(S^2{}_1 - S^1{}_1)\right) + r_{S_1^1}\ldots \quad (12)$$

$$dX^1{}_1/dt = (Q(1+R_1+R_2)/\alpha V_1)\left([X_i + X_2R_1 + X_{UF}R_2)/1+R_1+R_2] - X^1{}_1 + \beta(X^2{}_1 - X^1{}_1)\right) + r_{X_1^1}\ldots \quad (13)$$

For the anoxic reactor fraction with less agitated (concentrations are accented with 2):

$$dS^2{}_1/dt = (Q(1+R_1+R_2)\beta/(1-\alpha)V_1)(S^1{}_1 - S^2{}_1) + r_{S_1^2}\ldots \quad (14)$$

$$dX^1{}_1/dt = (Q(1+R_1+R_2)\beta/(1-\alpha)V_1)(X^1{}_1 - X^2{}_1) + r_{X_1^2}\ldots \quad (15)$$

For the aerobic reactor:

$$dS_2/dt = (Q(1+R_1+R_2)/V_2)(S^1{}_1 - S_2) + r_{S2}\ldots \quad (16)$$

$$dX_2/dt = (Q(1+R_1+R_2)/V_2)(X^1{}_1 - X_2) + r_{X2}\ldots \quad (17)$$

Table 3 Wastewater characteristics used in the simulations (Vanhooren and Nguyen, 1996)

Variable	Value
S_{Ii}[a]	30
S_{Si}[a]	70
X_{Ii}[a]	52
X_{Si}[a]	200
X_{BHi}[a]	28
X_{BAi}[a]	0.25
X_{Pi}[a]	5.0
S_{Oi}[b]	0.25
S_{NOi}[c]	0.25
S_{NHi}[c]	30.0
S_{NDi}[c]	7.0
X_{NDi}[c]	11.0
S_{ALKi}[d]	10.0

a: mg COD/L, mg of Chemical Oxygen Demand; b: mg O_2/L; c: mg N/L; d: mol/L

Table 4 Kinetic and stoichiometric parameters used in the simulation (Alex *et al*., 2008)

Parameter	Definition	Value
μ_H	Max. specific growth rate for Heterotrophs (d^{-1})	4.0
μ_A	Max. specific growth rate for Autotrophs (d^{-1})	0.5
K_S	Half saturation constant for Heterotrophs (mg COD/L)	10
K_{OH}	Half saturation constant for O_2 Heterotrophs (mg O_2/L)	0.2
K_{NO}	Half saturation constant for Heterotrophs (mg NO_3-N/L)	0.5
η_G	Correction for Anoxic Heterotrophic growth (-)	0.8
K_{OA}	Half saturation constant for O_2 Autotrophs (mg O_2/L)	0.4
K_{NH}	Half saturation constant for Autotrophic. (mg NH_3-N/L)	1.0
b_H	Decay constant for Heterotrophs (d^{-1})	0.3
b_A	Decay constant for Autotrophs (d^{-1})	0.05
k_a	Ammonification rate (l.COD/mg.d)	0.05
k_h	Max. specific Hydrolysis rate (mg COD/mg COD biomass.d)	3.0
K_X	Half saturation constant for Hydrolysis (mg COD/mg COD biomass)	0.1
η_h	Correction for Anoxic Hydrolysis (-)	0.8
y_H	Heterotrophic yield coefficient (mg biomass/mg COD)	0.67
y_A	Autotrophic yield coefficient (mg biomass/mg N)	0.24
f_p	Particulate yielding biomass fraction (-)	0.08
i_{XB}	Nitrogen fraction in biomass (mg N/mg COD biomass)	0.08
i_{XP}	Nitrogen fraction in biomass products (mg N/mg COD biomass)	0.06

2. Computer simulations

The performance of the PD-AS is simulated dynamically under ideal conditions (CSTR) and real conditions (CSTR with dead volume and two CSTRs with material exchange). The characteristics of treated wastewater are given in Table 3, the kinetic and stoichiometric parameters are given in **Table 4**. The group of ODEs representing the behavior of all constituents in the system where solved simultaneously in order to simulate the operation of the system for 30 days. The equations were solved using fourth-order Runge–Kutta procedure in MATLAB (The MathWorks Inc., Natick, MA), with a maximum time step of 1 day. The system's performance was evaluated by calculating the following constituents in the effluent (Alex *et al*., 2008):

A. Total Kjeldahl Nitrogen (Rittmann and McCarty, 2001) in effluent and waste (TKN_E and TKN_W):

$$TKN_E = S_{NH}^2 + X_{ND}^{OF} + i_{XB}(X_{BA}^{OF} + X_{BH}^{OF}) + i_{XP}(X_P^{OF} + X_I^{OF}) \quad (18)$$

$$TKN_W = S_{NH}^2 + X_{ND}^{UF} + i_{XB}(X_{BA}^{UF} + X_{BH}^{UF}) + i_{XP}(X_P^{UF} + X_I^{UF}) \quad (19)$$

B. Total Ammonia and Nitrate concentrations ($S_{NH\text{-}E}$ and $S_{NO\text{-}E}$).

C. Biochemical oxygen demanding (Rittmann and McCarty, 2001) organics in the effluent (BOD_E and BOD_W):

$$BOD_W = 0.25\left(S_S^2 + X_S^{UF} + (1-f)(X_{BA}^{UF} + X_{BH}^{UF})\right) \quad (21)$$

D. Chemical oxygen demanding (Rittmann and McCarty, 2001) organics in effluent and waste (COD_E and COD_W):

$$COD_E = S_I^2 + S_S^2 + X_I^{OF} + X_S^{OF} + X_{BA}^{OF} + X_{BH}^{OF} + X_P^{OF} \quad (22)$$

$$COD_W = S_I^2 + S_S^2 + X_I^{UF} + X_S^{UF} + X_{BA}^{UF} + X_{BH}^{UF} + X_P^{UF} \quad (23)$$

To study the system performance under real conditions, multiple simulations were performed while varying the values of the two parameters in the real reactor models in order to reflect varying degrees of nonideal flow: For the CSTR with dead volume model, α was changed from 1 to 0.1, while β was changed from 0 to 0.9, and for the two CSTRs with exchange model α was changed from 0.9 to 0.1, while β was changed from 0.01 to 0.9. The aforementioned values for α and β were chosen to depict a moderate, intermediate, and extreme non-ideal flow scenarios.

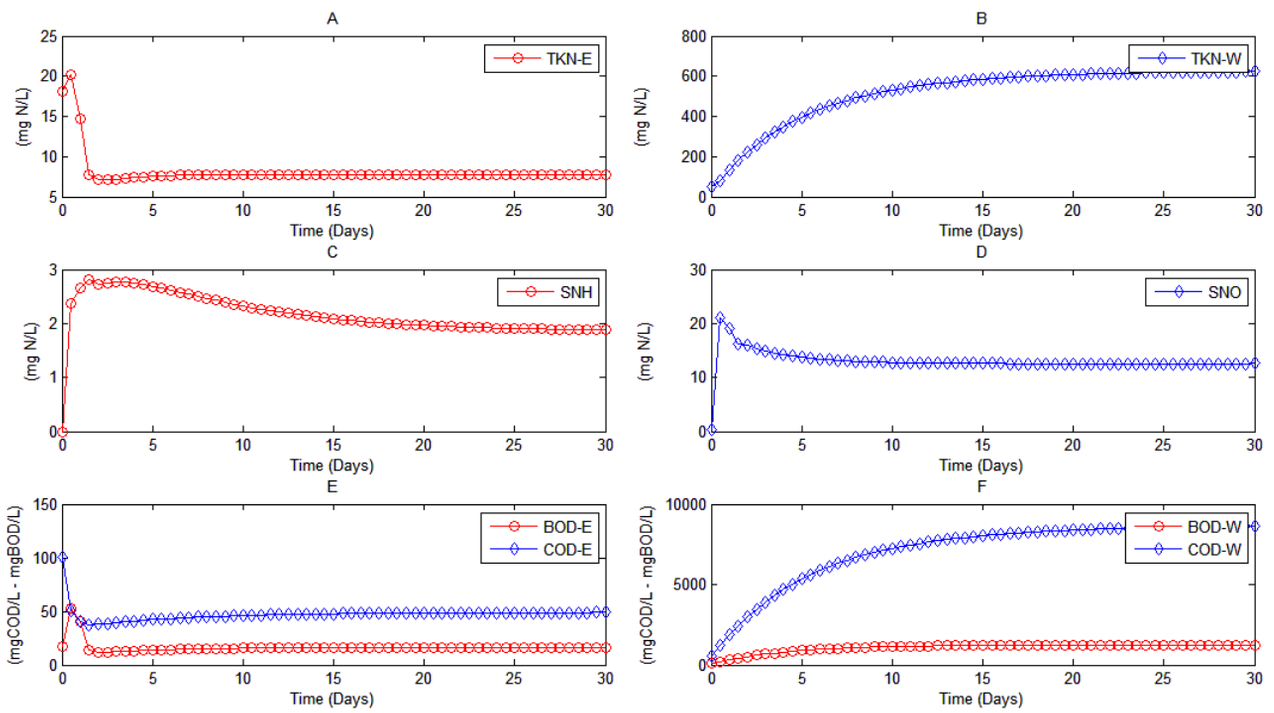

Fig. 3 PD-AS performance under ideal mixing condition; A: TKN_E, B: TKN_W, C: $S_{NH\text{-}E}$, D: $S_{NO\text{-}E}$, E: BOD_E and COD_E, and F: BOD_W and COD_W.

3 Results and Discussion

3.1 Ideal completely mixed reactors

The PD-AS system operation was simulated for 30 days. **Figure 3** shows the system performance as a function of time. Effluent steady-state S_{NH} , S_{NO}, and TKN_E concentrations were 1.8, 12.5, and 3.9 mg N/L, respectively, while BOD_E and COD_E were 16.4 mg/L and 48.9 mg/L, respectively. The daily waste included 626 mg N/L of TKN , 1271 mg/L of BOD, and 8625 mg/L of COD. The simulation outcome was comparable to other published simulations results for similar PD-AS reactor sizes and feed wastewater composition (Alex *et al*., 2008).

3.2 CSTR with bypass and dead volume

Figure 4 shows the effect of varying the non-ideal mixing parameters on the concentration of nitrogen compounds in the system. As can be seen, the system's effluent TKN concentration varied marginally with increasing mixing non-idealities (**Figure 4A**) (i.e. increased bypass fraction and dead volume fraction). This can be attributed to the fact that effluent TKN is mainly soluble, and removed in the aerobic reactor, where mixing performance was assumed ideal.

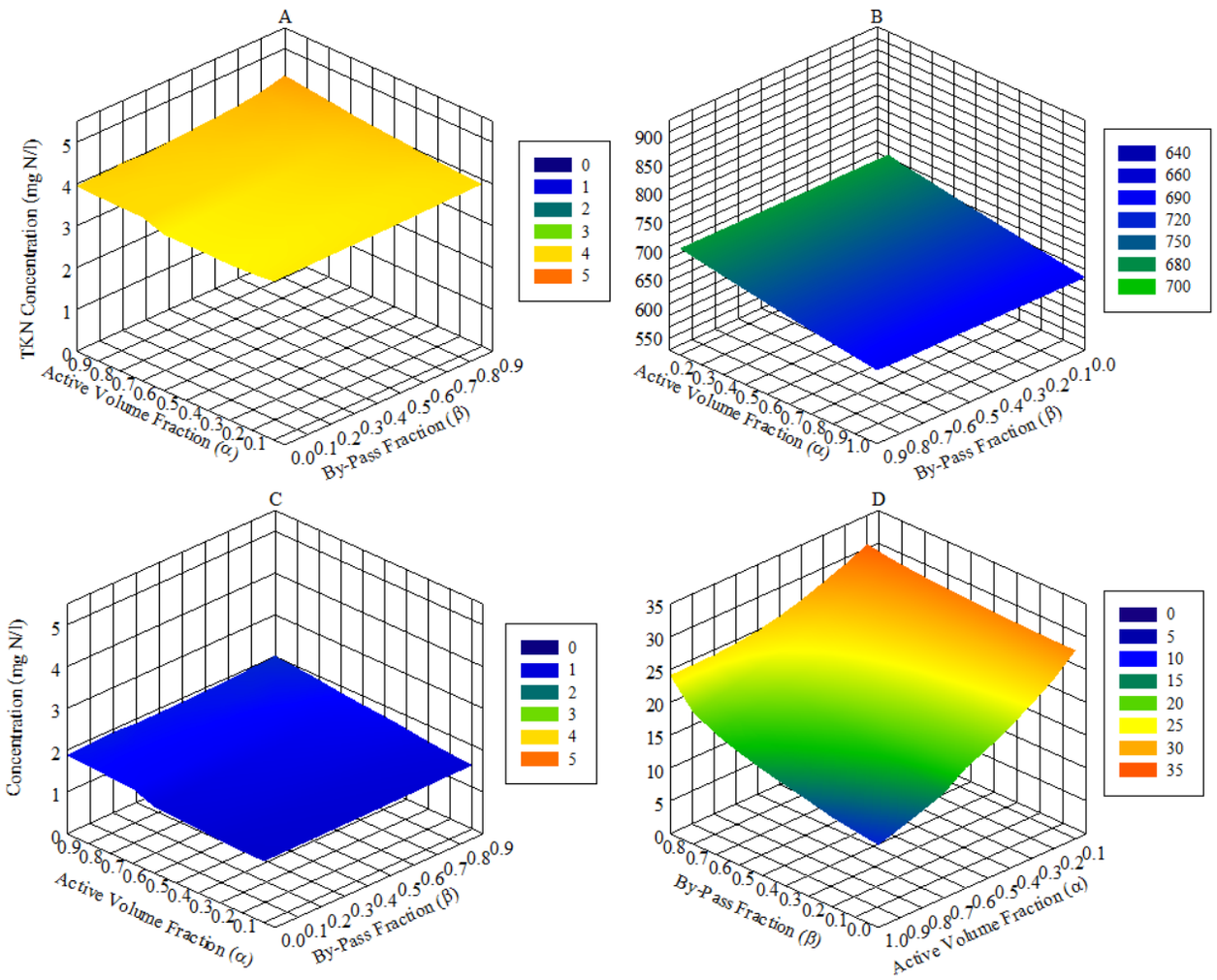

Fig. 4 Simulated PD-AS nitrogen related performance under CSTR with bypass/dead volume non-ideal mixing effects at $0.1 \leq \alpha \leq 1.0$ and$0 \leq \beta < 0.9$; A: TKN_E, B: TKN_W, C: $S_{NH\text{-}E}$, and D: $S_{NO\text{-}E}$.

The same trend was noticed for the total ammonia in the effluent, which remained relatively constant (**Figure 4C**). TKN_W increased with increasing mixing non-idealities, as can be seen in **Figure 4B**. This is attributed to the increase in the heterotrophic biomass in the system (from 2570 to 2980 mg COD/L) as a result of the increase in substrate availability in the aerobic reactor brought by the increase in bypass ratio. The TKN_W increase may affect anaerobic treatment for the wasted biomass (Chen *et al*., 2008; Tezel *et al*., 2014), due to the elevated levels of nitrogen. On the other hand, the effluent nitrate concentration increased drastically as the system was shifted towards non-ideal mixing conditions. As seen in Fig. 4C, $S_{NO\text{-}E}$ exceeded 20 mg N/L at $\alpha \leq 0.4$ and $\beta \leq 0.4$. The decrease in α (increase in dead volume fraction) had a larger effect on $S_{NO\text{-}E}$ compared to β. Similar performance short comes were observed by Manenti *et al*. (Manenti *et al*., 2018), when the actual retention time failed in assuring an acceptable treatment level below a minimum threshold value. Collivignarelli (Collivignarelli *et al*., 2018) reported that reducing the dead volume fraction will result in an enhancement of nitrate removal, while Kjellstr and co-researchers (Kjellstrand *et al*., 2005) reported that the presence of a dead volume in the reactor will reduce the denitrifying capacity due to reduced active volume, and high nitrate concentration in the effluent can appear due to the short-circuiting stream (bypass). **Figure 5** shows the effect of varying the non-ideal mixing parameters on the concentration of BOD and COD in the system. As seen in **Figure 5A** and **Figure 5B**, increasing mixing non-idealities had a slight effect on BOD_E and COD_E. However, as with $S_{NO\text{-}E}$, decreasing α had the main effect. This can be attributed to the reduction in the anoxic reactor's active volume size, leading to a lesser conversion due to smaller real retention times (Fogler, 1999). This connects to the increase in $S_{NO\text{-}E}$ as seen in **Figure 4D** since (as mentioned in section 1) nitrite is utilized exclusively by the heterotrophic biomass organic carbon mineralization in the anoxic reactor.

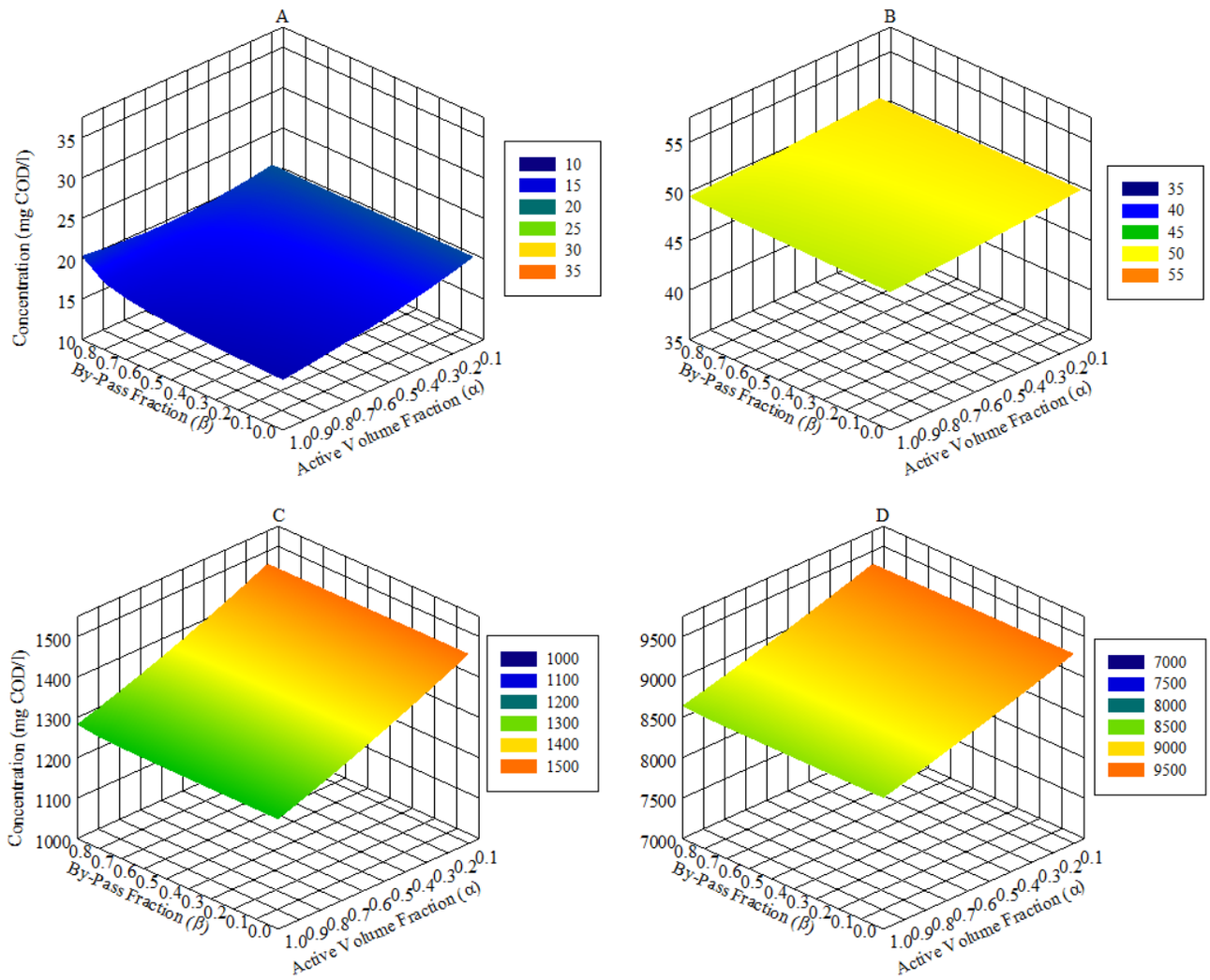

Fig. 5 Simulated PD-ASorganic carbon-related performance under CSTR with bypass/dead volume non-ideal mixing effects at $0.1 \leq \alpha \leq 1.0$ and$0 \leq \beta < 0.9$; A: BOD_E, B: COD_E, C: BOD_W, and D: COD_W.

As seen in Fig. 5C and Fig. 5D, both of BOD_W and COD_W concentrations increased in the waste stream as a direct response to increased biomass in the system, which was brought by the greater than before availability of substrate in the aerobic reactor due to increased bypass fraction and decreased active volume fraction in the anoxic reactor. Collivignarelli (Collivignarelli *et al*., 2018) reported that reducing the dead volume fraction will enhance COD and BOD. The increase in the concentrations of BOD_W and COD_W in the waste stream, coupled with the increase of TKN_W, will amplify the load on waste disposal facilities in the wastewater treatment plant. Similar to what has been observed with $S_{NO\text{-}E}$ above, the active volume fraction (α) had a larger effect on the system's *BOD* and *COD* concentrations when compared to the bypass fraction. It must be added that, apart from nitrate concentration, the resulting changes in the PD-AS's performance were related to particulate constituents in the system. However, their concentration in the system is directly correlated with the settler's performance (i.e. *SE* value). The SE value was assumed constant to eliminate the effect of the settler's performance on the predicted outcome.

3.3 Two CSTRs with material exchange

As mentioned in section 2.3.2, this model describes a scenario where the mixing apparatus in the anoxic reactor are poorly positioned, resulting in rapid mixing in their vicinity, while the remaining region undergoes mixing, albeit at a lesser rate. Carried out simulations for the system's operation at the current non-ideal mixing scenario showed that, to some extent, its performance was unaffected. This was in a specific range of the mixing model α and β values: $0.4 \leq \alpha \leq 0.9$ and$0.1 \leq \beta \leq 0.9$. Table 5 shows the unaffected system's performance. **Figure 6** and **Figure 7** shows the performance of the system beyond the abovementioned range for the mixing model parameters values (i.e. second range at $0.1 \leq \alpha < 0.4$ and$0.01 \leq \beta < 0.1$). It is clear that the system's effluent TKN concentration slightly (**Figure 6A**) varied with increasing mixing non-idealities within the second range (i.e. reducing the rapid agitation zone and material exchange fractions). This took place because *TKN* is mainly removed in the aerobic reactor, which its mixing performance was assumed ideal. The relatively constant total ammonia in the effluent (**Figure 6C**) suggests that that ammonia removal is

unaffected.

Table 5 Effluent constituents of the PD-AS system with and without ideal mixing conditions

Effluent Constituents	Ideal mixing	CSTRs with material exchange
TKN_E	3.9 mg N/L	3.9±0.09[a]mg N/L
TKN_W	626.5 mg N/L	628.5±4.8mg N/L
$S_{NH\text{-}E}$	1.9 mg N/L	1.8±0.05mg N/L
$S_{NO\text{-}E}$	12.6 mg N/L	14.1±1.2mg N/L
BOD_E	16.2 mg BOD/L	16.7±0.9 mg BOD/L
COD_E	48.9 mg COD/L	49.1±0.2 mg COD/L
BOD_W	1271.9 mg BOD/L	1278.8±15.2 mg BOD/L
COD_W	8625.6 mg COD/L	8652.3±61.5 mg COD/L

a: Average ± Standard Deviation.

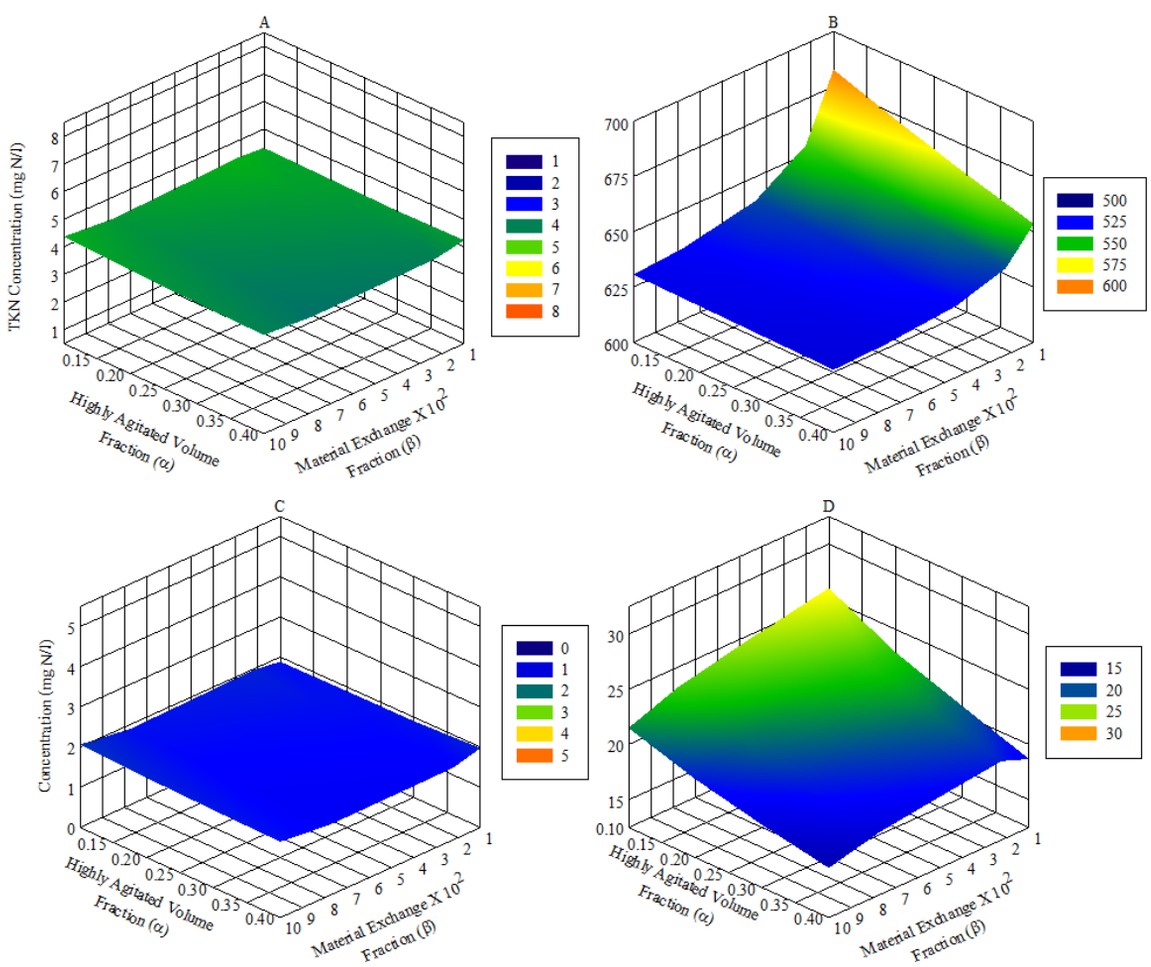

Fig. 6 Simulated PD-AS nitrogen related performance under the 2 CSTRs with material exchange non-ideal mixing effects at $0.1 \leq \alpha < 0.4$ and$0.01 \leq \beta < 0.1$; A: TKN_E, B: TKN_W, C: $S_{NH\text{-}E}$, and D: $S_{NO\text{-}E}$.

However, the TKN_W (which is mainly comprised from particulates) increased with increasing mixing non-idealities (**Figure 6B**), but only at extreme non-ideal mixing condition, when the anoxic reactor volume was mostly affected by low mixing due to very slow agitation ($\alpha < 0.3$ and $\beta < 0.01$). Operation within this range also increased the heterotrophic biomass in the system (from 2570 to 2708±136 mg COD/L), due to ineffective utilization of readily biodegradable organic carbon in the anoxic reactor (S_S+X_S increased in

the anoxic reactor effluent from 82.2 to 117±12mg COD/L), and were utilized by the aerobic reactor. Similar to the dead volume/bypass model, the increase TKN_W concentration and biomass concentration in the waste stream may affect anaerobic treatment processes for the wasted biomass. The effluent nitrate concentration increased drastically as the system was shifted towards extreme non-ideal mixing conditions. As seen in Fig. 6C, $S_{NO\text{-}E}$ exceeded 20mg N/L at $\alpha < 0.2$ and $\beta < 0.01$. This behavior mimicked the result seen in the dead volume/bypass model, however at more extreme non-ideal mixing conditions in this model. The increase is probably a result of the anoxic reactor's active volume becoming extremely low (i.e. fast residence times), not permitting any effective reactions. This can be connected to the increase of readily biodegradable organic carbon in the anoxic reactor (see before), being not utilized fully under these conditions. Results shown in Fig. 6 showed that the system's performance was more affected by the high agitation fraction (α). Fig. 7 shows the effect of varying the nonideal mixing parameters on the concentration of BOD and COD in the system.

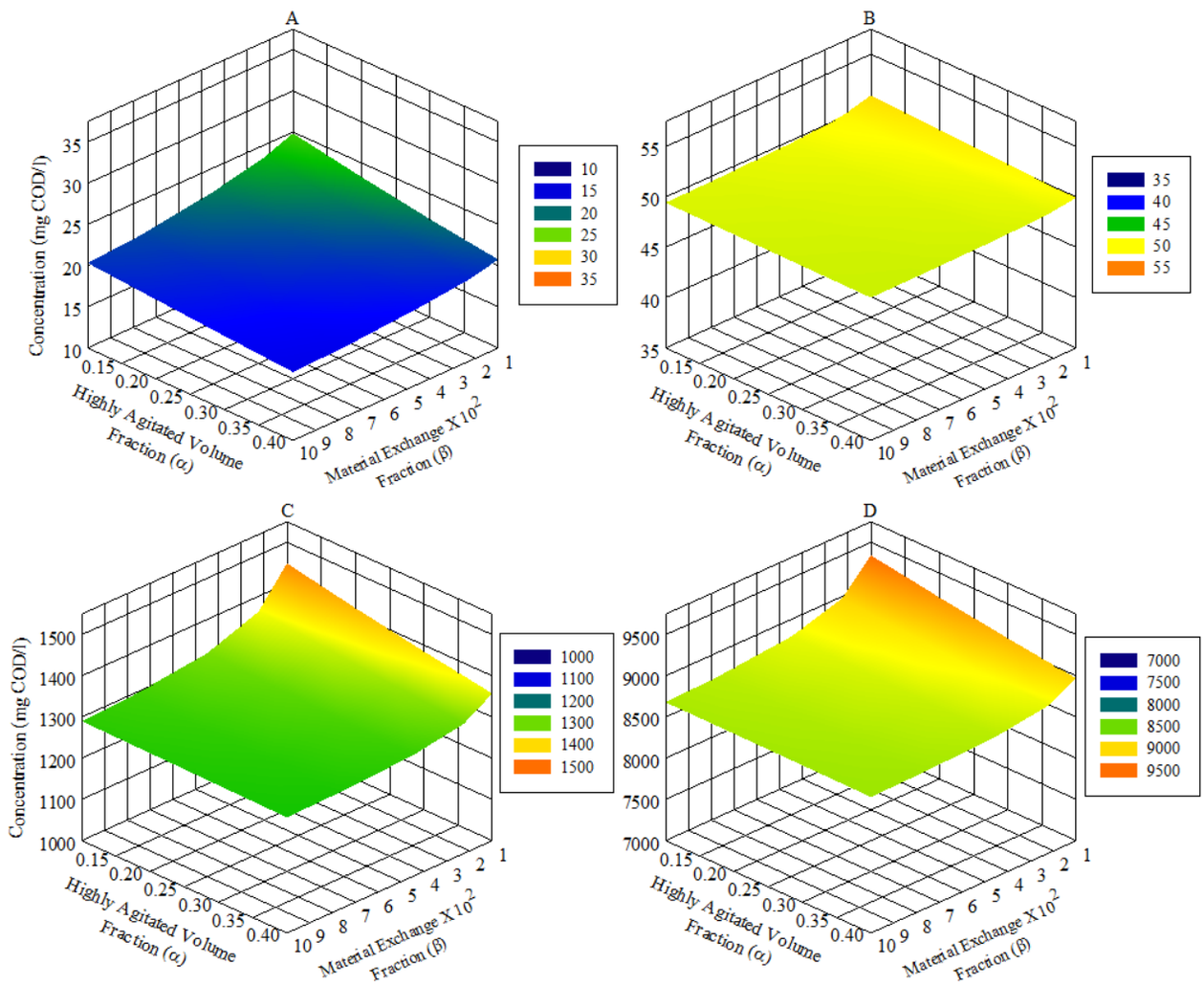

Fig. 7 Simulated PD-AS nitrogen related performance under the 2 CSTRs with material exchange non-ideal mixing effects at $0.1 \leq \alpha < 0.4$ and$0.01 \leq \beta < 0.1$; A: TKN_E, B: TKN_W, C: $S_{NH\text{-}E}$, and D: $S_{NO\text{-}E}$.

As seen in Fig. 7.A and Fig. 7.B, only extreme levels of mixing non-idealities had an effect on BOD_E and COD_E. The increase is probably related to the increased heterotrophic biomass in the system (from 2570 to 2708±136 mg COD/L), due to ineffective utilization of readily biodegradable organic carbon in the anoxic reactor. As seen in Fig. 7.C and Fig. 7.D, both of BOD_W and COD_W concentrations increased in the waste stream as a direct response to increased biomass in the system, which was brought by the greater than before availability of substrate in the aerobic reactor due to reduced active anoxic reactor volume. The increase in the concentrations of BOD_W and COD_W in the waste stream will amplify the load on waste disposal facilities in the wastewater treatment plant. The aforementioned results showed that the system's performance was more affected by the high agitation fraction (α). Results shown in Figs. 6 and**7** showed that the non-ideal mixing scenario depicted by the two CSTRs with the material exchange had minor effects on the performance of the PD-AS system. Even so, these effects occurred at extreme non-ideal situations. However, this stipulation could be related to the specific operating conditions of the PD-AS under investigation. Moreover, previously published work suggests that increasing the number of CSTRs (i.e. compartments) in this model could provide a more representative depiction of the mixing non-idealities in AS systems (Liotta *et al*., 2014).

Conclusions

The system's performance was largely affected by the presence of a dead volume/bypass scenario compared to the two mixing zones with a material exchange scenario. Under non-ideal mixing conditions, effluent concentrations of Total Kjeldahl Nitrogen, organic carbon increased marginally. On the other hand, the effluent concentration of nitrate increased significantly under the same conditions, indicating a reduction in nitrate removal efficiency. The heterotrophic biomass concentration in the system increased under non-ideal mixing conditions. This by its part resulted in an increase in the waste stream concentrations of Total Kjeldahl Nitrogen and organic carbon. This study provides an insight into the behavior of pre-denitrification activated sludge systems when affected by non-ideal mixing conditions. Additionally, it identified some performance discrepancies that could-if found in a real system-indicate the presence of a dead volume/bypass or two mixing zones mixing non-idealities in the anoxic reactor.

Nomenclature

Acronyms

AS	=Activated Sludge
PD	=Pre-Denitrification
CSTR	=Continuous stirred-tank reactor
SE	=particulates separation coefficient
COD	=Chemical Oxygen Demand
BOD	=Biochemical Oxygen Demand
TKN	=Total Kjeldahl Nitrogen
E	=Effluent
W	=Waste
UF	=Underflow
OF	=Overflow

Symbols

S	=Dissolved material concentration	[mg COD/L]
S_i	=Dissolved material concentration in the feed	[mg COD/L]
S_I	=Soluble inert organics concentration	[mg COD/L]
S_S	=Readily biodegradable (soluble) substrate concentration	[mg COD/l]
X	=particulate material concentration	[mg COD/L]
X_i	=Particulate material concentration in the feed	[mg COD/L]
X_I	=Particulate inert organics concentration	[mg COD/L]
X_S	=Slowly biodegradable (particulate) concentration	[mg COD/L]
X_{BH}	=Active heterotrophic biomass concentration	[mg COD/L]
X_{BA}	=Active autotrophic biomass concentration	[mg COD/L]
X_P	=Non-biodegradable particulates from cell decay concentration	[mg COD/L]
S_O	=Dissolved oxygen concentration	[mg O_2/L]
S_O^{SAT}	=Saturation dissolved oxygen concentration	[mg O_2/L]
S_{NO}	=Nitrate concentration	[mg N/L]
S_{NH}	=Free and ionized ammonia concentration	[mg N/L]
S_{ND}	=Soluble biodegradable organic nitrogen concentration	[mg N/L]
X_{ND}	=Particulate biodegradable organic nitrogen concentration	[mg N/L]
S_{ALK}	=Alkalinity	[mol/L]
K_L	=Oxygen transfer coefficient	[d^{-1}]
Q	=Feed wastewater flow rate	[m^3/d]
Q_W	=Waste flow rate	[m^3/d]
R_1	=Nitrate recycle ratio	[-]
R_2	=Solids recycle ratio	[-]
V_1	=Anoxic reactor volume	[m^3]
V_2	=Aerobic reactor volume	[m^3]
r	=Reaction rate	[mg/L.d]
K_S	=Half saturation constant for Heterotrophs	[mg COD/L]
K_{OH}	=Half saturation constant for O_2 Heterotrophs	[mg O_2/L]
K_{NO}	=Half saturation constant for Heterotrophs	[mg NO_3-N/L]
K_{OA}	=Half saturation constant for O_2 Autotrophs	[mg O_2/L]
K_{NH}	=Half saturation constant for Autotrophic	[mg NH_3-N/L]
b_H	=Decay constant for Heterotrophs	[d^{-1}]
b_A	=Decay constant for Autotrophs	[d^{-1}]
k_a	=Ammonification rate	[L.mg COD/mg.d]
k_h	=Max. specific Hydrolysis rate	[mg COD/mg COD.d]
K_X	=Half saturation constant for Hydrolysis	[mg COD/mg COD]
y_H	=Heterotrophic yield coefficient	[mg biomass/mg COD]
y_A	=Autotrophic yield coefficient	[mg biomass/mg N]
f_p	=Particulate yielding biomass fraction	[-]
i_{XB}	=Nitrogen fraction in biomass	[mg N/mg COD biomass]
i_{XP}	=Nitrogen fraction in biomass products	[mg N/mg COD biomass]

Greek letters

α	=Non-ideal mixing parameter 1	[-]
β	=Non-ideal mixing parameter 2	[-]
μ_H	=Max. specific growth rate for Heterotrophs	[d^{-1}]
μ_A	=Max. specific growth rate for Autotrophs	[d^{-1}]
η_G	=Correction for Anoxic Heterotrophic growth	[-]
η_h	=Correction for Anoxic Hydrolysis	[-]

References

Alex, J., Benedetti, L., Copp, J., Gernaey, K., Jeppsson, U., Nopens, I., Pons, M., Rieger, L., Rosen, C., and Steyer, J. "Benchmark simulation model no. 1 (bsm1)", *Report by the IWA Taskgroup on Benchmarking of Control Strategies for WWTPs* (2008).

Badkoubi, A., Ganjidoust, H., Ghaderi, A., and Rajabi, A. "Performance of a subsurface constructed wetland in Iran", *Water Sci. and Tech.*, **38**, 345-350 (1998).

Chen, Y., Cheng, J., and Creamer, K. "Inhibition of anaerobic digestion process: A review", *Biores. Tech.*, **99**, 4044-4064 (2008).

Collivignarelli, M., Bertanza, G., Abbà, A., and Damiani, S. "Troubleshooting in a full-scale wastewater treatment plant: What can be learnt from tracer tests", *Int. J. of Env. Sci. and Tech.*, 1-12 (2018).

Copp, J. "The cost simulation benchmark: Description and simulator manual: A product of cost action 624 and cost action 682", *EUR-OP* (2002).

Fogler, H. "Elements of chemical reaction engineering", Upper Saddle River, New Jersey, *Pearson Education, Inc.*, (1999).

García, J., Aguirre, P., Barragán, J., Mujeriego, R., Matamoros, V., and Bayona J. "Effect of key design parameters on the efficiency of horizontal subsurface flow constructed wetlands", *Eco. Eng.*, **25**, 405-418 (2005).

Hajaya, M.G., and Pavlostathis S. "Modeling the fate and effect of benzalkonium chlorides in a continuous-flow biological nitrogen removal system treating poultry processing wastewater", *Biores. Tech.*, **130**, 278-287 (2013).

Hellinga, C., van Loosdrecht, M., and Heijnen J. "Model based design of a novel process for nitrogen removal from concentrated flows", *Math. and Comp. Model. of Dyn. Sys.*, **5**, 351-371 (1999).

Henze, M., Gujer, W., Mino, T., and Van Loosdrecht, M. "Activated sludge models asm1, asm2, asm2d and asm3", *IWA publishing* (2000).

Kim, H., Noh, S., and Colosimo, M. "Modeling a bench-scale alternating aerobic/anoxic activated sludge system for nitrogen removal using a modified asm1", *J. of Env. Sci. and Heal. Part a-Toxic/Hazardous Substances & Environmental Engineering*, **44**, 744-751 (2009).

Kjellstrand, R. "Hydraulic behaviour in an activated sludge tank: From tracer test through hydraulic modelling to full-scale implementation" [Dissertation], Göteborg: Chalmers tekniska högskola, (2006)

Kjellstrand, R., Mattsson, A., Niklasson, C., and Taherzadeh, M. "Short circuiting in a denitrifying activated sludge tank", *Water Sci. and Tech.*, **52**, 79-87 (2005).

Le Moullec, Y., Gentric, C., Potier, O., and Leclerc, J. "Comparison of systemic, compartmental and cfd modelling approaches: Application to the simulation of a biological reactor of wastewater treatment", *Chem. Eng. Sci.*, **65**, 343-350 (2010).

Le Moullec, Y., Potier, O., Gentric, C., and Leclerc, J. "Activated sludge pilot plant: Comparison between experimental and predicted concentration profiles using three different modelling approaches", *Water Res.*, **45**, 3085-3097 (2011).

Liotta, F., Chatellier, P., Esposito, G., Fabbricino, M., Van Hullebusch, E., and Lens P. "Hydrodynamic mathematical modelling of aerobic plug flow and nonideal flow reactors: A critical and historical review", *Crit.l Rev. in Env. Sci. and Tech.*, **44**, 2642-2673 (2014).

Madigan, M. T., and. Martinko, J "Brock biology of microorganisms ", Upper Saddle River, NJ, *Pearson Prentice Hall* (2006).

Manenti, S., Todeschini, S., Collivignarelli, M., and Abbà, A. "Integrated rtd− cfd hydrodynamic analysis for performance assessment of activated sludge reactors", *Env. Proc.*, **5**, 23-42 (2018).

Ostace, G., Cristea, V., and Agachi P. "Cost reduction of the wastewater treatment plant operation by mpc based on modified asm1 with two-step nitrification/denitrification model", *Comp. and Chem. Eng.*, **35**, 2469-2479 (2011).

Pereira, J., Karpinska, A., Gomes, P., Martins, A., Dias, M., Lopes, J., and Santos R. "Activated sludge models coupled to cfd simulations", *Single and two-phase flows in chemical and biomedical engineering*, **153**, 153-173 (2012).

Rittmann, B., and McCarty, P. "Environmental biotechnology: Principles and applications", New York, NY, *McGraw-Hill* (2001).

Sánchez, F., Viedma, A., and Kaiser A."Hydraulic characterization of an activated sludge reactor with recycling system by tracer experiment and analytical models", *Water Res.*, **101**, 382-392 (2016).

Tchobanoglous, G., Burton, F., and. Stensel, H. "Wastewater engineering: Treatment and reuse", New York, NY, *McGraw-Hill Professional* (2007).

Tezel, U., Tandukar, M., Hajaya, M., and Pavlostathis, S. "Transition of municipal sludge anaerobic digestion from mesophilic to thermophilic and long-term performance evaluation", *Biores. Tech.*, **170**, 385-394 (2014).

Van Loosdrecht, M., Lopez-Vazquez, C., Meijer, S., Hooijmans, C., and Brdjanovic, D."Twenty-five years of asm1: Past, present, and future of wastewater treatment modelling", *J. of Hydro.*, **17**, 697-718 (2015).

Vanhooren, H., and Nguyen, K. "Development of a simulation protocol for evaluation of respirometry-based control strategies", *Report University of Gent and University of Ottawa* 1996).

Vanrolleghem, P., Insel, G., Petersen, B., Sin, G., De Pauw, D., Nopens, I., Dovermann, H., Weijers, S., and Gernaey, K."A comprehensive model calibration procedure for activated sludge models", *Proc. of the Water Env. Feder.*, **2003**, 210-237 (2003).

Utilization of Volcanic Tuffs as Construction Materials

Kamel Al-Zboon[1], Jehad Al-Zou'by[1] , Ziad Abu-Hamatteh[2]

[1)] *Environmental Engineering Department, Al-Huson University College, Al-Balqa Applied University, Irbid, Jordan.*
[2)] *Civil Engineering Departments, Faculty of Engineering Technology, Al-Balqa Applied University, Amman, 11134 Jordan*

The current study examines the possibility of utilizing the Jordanian volcanic tuff aggregates as a source of many construction materials. Different mixtures were prepared by replacing the commonly used normal aggregate with volcanic tuffs aggregate to determine the best mixing proportion with similar size in different ratios as 0, 25, 50, 75 and 100%. The impacts of this replacement on brick's compression strength, dry weight and water absorption, transverse strength, absorption and weight of terrazzo tiles, loss Anglos and CBR values have been examined and evaluated. The results revealed an improvement in compressive strength of bricks at a replacement ratio of 25%, with concomitant reduction at higher replacement ratios, while water absorption increased as the ratio of tuff increases. Transverse strength of terrazzo tiles was recorded as 6.08, 5.78, 5.78, 5.21 and 5.19 MPa at substitution ratios of 0, 25, 50, 75 and 100%, respectively. Utilization of volcanic tuffs resulted in a significant reduction in the dry weight of bricks and terrazzo provided lightweight material. CBR test indicated that this material can be used successfully in foundations and as a sub-base material. The obtained results buttressed the benefit of utilization of natural volcanic tuffs as construction materials.

Keywords: Volcanic Tuffs, Construction Materials, Terrazzo Tiles, Bricks, Pavement Materials, Jordan.

Introduction

Selection and preparation of construction materials are of prime importance in all major engineering projects, including road pavements, concrete mixes and other construction materials such as tiles and bricks. The engineering properties of the construction materials are supposed to meet the standards in order to achieve the minimum requirements in terms of strength and durability. (Bell, 2007). The selection of construction materials basically depends on the common index properties of rocks, such as durability, strength, density permeability, and porosity. Other interference conditions such as climate conditions, project purposes and cost-effectiveness should be considered during the selection and preparation process of the construction materials. The utilization of the local construction materials while maintaining the required properties and specifications represent a challenge for civil engineering all over the world (McLean and Gribble, 2005; Rahn, 1996; Johnson and DeGraff 1988). In light of the overpoweringly increasing demand for raw materials by various construction, sectors created a serious shortage in some building materials. Therefore, in order to meet the dramatically increasing demand, uncommon sources of such materials with acceptable engineering properties becomes precedence. Volcanic tuff (VT) is considered as a promising source of natural construction materials. Volcanic tuff, one of the most important natural pozzolan materials, has been used since ancient times in buildings, bridges, walls, and masonry works. Currently, it is used in many countries in the world for masonry mortars, lightweight concretes and thermal for acoustic insulation materials (Balog *et al*., 2014). Volcanic tuff with its unique structure and unique properties could serve as a construction material in many engineering projects. Tuff is a relatively soft, high porous with high surface area and low-density igneous rock formed from volcanic ash or dust (Al-Zboon and Al-Zou'by, 2017). It is considered as a good inexpensive source for lightweight aggregate concrete leading to a considerable cost saving in various construction materials (Turkmenoglu and Tankut 2002; Negis, 1999; Kılınçarslan, 2011). The feasibility of using volcanic tuff as a light-weight aggregate in cement and concrete industry has been reported by many researchers (Turkmenoglu and Tankut 2002; Al-Zboon and Al-Zou'by, 2017; USBR, 1992; Kan and Gul, 1996; Kılıc *et al*., 2009; Augenti and Parisi, 2010; Faella *et al*., 1992; Smadi and Migdady, 1991; Kavasa and Evcin, 2005; Abali *et al*., 2006). The specific gravity of VT is about 1.84, while it is about 2.52 for ordinary sand. For this reason, VT can provide lightweight concrete with a density of 1440-1840kg/ m^3 in comparison with 2400kg/m^3 for normal aggregate concrete (Fredrick, 2014). Al-Zboon and Al-Zou'by (2017) used VT for concrete production and the results showed significant improvement in compressive and flexural strength at a replacement ratio of 25%, with reductions at higher ratios. Al-Zou'by and Al-Zboon (2014) utilized VT in cement mortar and found that a replacement ratio of 50% enhanced compressive strength and flexural strength. Yasin *et al*., (2012) studied the Jordanian tuffs for use in concrete production and they replaced 20% of the fine aggregates by volcanic tuff and thereby the concrete compressive strength improved significantly. Moreover, Fredrick (2014) replaced normal sand with VT in concrete mixes and reported an increase in the compressive strength of concrete cubes with 2.8%, 7.4%, 11.1% and 14.0% and 5.0% for replacement ratios of 20%, 40%, 60%, 80%, and 100%. In contrast, tensile strength decreased by 18.0%, 12.4%, 9.6%, 10.8% and increased (1.2%) for the same ratios respectively. Also, Smadi and Migdadi (1991) used successfully VT to produce high strength lightweight concrete and achieved high compressive strength as high as 60 MPa at 90 days. Limitations of using VT in concrete mixes include but not limited to the high water absorption (11.5%), high bleeding (28ml) and low slump value (<10mm) (Al-Zboon and Al-Zou'by, 2017).

Received on February 27, 2019; accepted on April 16, 2019. Correspondence concerning this article should be addressed to Ziad Abu-Hamatteh (E-mail address: hamatteh@bau.edu.jo). ORCID ID for Ziad Abu-Hamatteh: https://orcid.org/0000-0003-0929-1011

Al Dwairi *et al*., 2018 found that the replacement of normal limestone with volcanic tuff in concrete mixture resulted in an increase in compressive strength, modulus of rupture, shear stress, and flexural strength, while splitting strength decreased as the ratio of tuff increase. They concluded that the Jordanian tuff could be used as a lightweight concrete with good slump and absorption characteristics. Ababneh and Matalkah (2018) investigated the possible utilization of Jordanian volcanic tuff as a cementation material, and they found that JVT with high SiO_2, enhanced the compressive strength of mortars at early age (7days), while low replacement level provided better compressive strength at later age. Jordan has a huge reserve of VT mainly in the northeastern part, and a certain amount is more than two billion tons (MEMR, 2015). Nowadays, VT is used in Jordan in limited applications such as in cement production (about 400,000 ton/year), lightweight concrete and in the agricultural sector. The aim of the current investigation is to evaluate the possibility of using the Jordanian VT in the production terrazzo bricks, tiles, and pavement materials applying different ratios of VT to normal aggregates (NA). Previous studies have used limited particle size fractions of VT, whereas, the current study utilized as high as up to 100% and low down to 0% ratios of volcanic tuff as an attempted to achieve the best results. To the best of the author's knowledge, this is the first time, that Jordanian tuff is used to produce bricks, terrazzo tiles and as a basement material.

2 Materials and Methods

2.1 Materials and batching

Normal aggregate was replaced with the same size of VT at different ratios (**Table 1**), namely: B_2 (25% VT), B_3 (50%VT), B_4 (75% VT) and B5 (100%VT), in addition to the control B1 (0% VT). The properties of VT have been determined previously (Al-Zboon and Al-Zou'by, 2017), where the oven-dry specific gravity ranged from 1.96 to 1.82 with absorption ratio of 10.1 and 11.5% for coarse and fine VT, respectively. For NA, the specific gravity ranged from 2.6 to 2.55 with absorption ratio of 1.2 to 1.7% for coarse and fine NA, respectively. Constant rate of Portland cement (200kg/m^3) was added to the aggregate component of the mix (NA and VT) and all are blended in a dry condition. Also, a constant amount of water (190kg/m^3) was gradually added to the mixture to achieve homogeneity and plastic form. A Mechanical mixer with a volume of 0.2m^3 was used for mixing the components for the required time of 5minutes.

Table 1 Volcanic tuff and aggregate ratios in different mixture proportions.

Batch	B_1	B_2	B_3	B_4	B_5
Percent of tuff (%)	0	25	50	75	100
Percent of normal aggregate (%)	100	75	50	25	0
Weight of tuff (kg)	0	72.5	145	217.5	290
Weight of normal aggregate (kg)	290	217.5	145	172.5	0
Weight of water (kg)	18	18	18	18	18
Weight of cement (kg)	19	19	19	19	19
Total (kg)	327	327	327	327	327

2.2 Molding and curing

At the end of mixing time, the mixture was poured in a container with enough size. Then, the mixture was transferred to the steel mold with an internal dimension of 40x20x15cm. When the mold is full of the mixture, it is subjected to mechanical vibration and compaction hydraulic force which resulted in high density and high strength. The compacted bricks are out of the molds and put on a clean, elevated surface and labeled with the required information includes the type of batch (B_1, B_2,…) and date of production. After drying for 24 hours, bricks were sprinkled with water for three days and then transferred to the storage for curing area according to the Jordanian standard N. 603/2 (MPWH, 1985). Twenty-four samples of bricks were taken for each mixing ratio B_1, B_2, and B_3, while only six samples were taken for B_4 and B_5 because the samples failed and did not form as required and the material threw out after de-molding.

2.3 Laboratory tests

Upon completing the 28 days incurring period, the bricks samples were analyzed in terms of density and compressive strength according to the standard method, ASTM C67 / C67M-18. In the lab, the samples were left for one hour for drying their surface, then dimensions and void area of bricks were determined. Initial absorption ratio was determined for three samples of each batch using oven-dried to equilibrium. The compressive strength of brick samples is determined using the hydraulic compression test machine has a maximum capacity of 2000 kN and capable to apply constant loading rate. Test procedure and speed of testing was conducted following ASTM C-67. The compressive strength of bricks was determined using the following equation:

$$F=P/A \quad (1)$$

Where F is the compressive strength (kN/cm^2), P is the applied force (KN), and A is the cross-sectional area (cm^2) of the brick in contact with the applied force.

2.4 Utilization of volcanic tuff in formulation of terrazzo tiles

Volcanic aggregates were added to the standard mixture with different ratios (**Table 2**). Except for the tuff content, the other parameters were kept constant for all batches including cement and water content, cement: aggregate ratio, quartz content of the top layer and mixing time. NA, VT, and cement were blended in a dry phase to achieve materials homogeneity, then water was added gradually with continuous mixing until achieving homogenous form (about 4 minutes).

Table 2 Materials used for different batches of terrazzo tiles.

Batch	T_1	T_2	T_3	T_4	T_5
Percent of tuff (%)	0	25	50	75	100
Percent of normal aggregate (%)	100	75	50	25	0
Dimension of tiles (cm)	30*30*3	30*30*3	30*30*3	30*30*3	30*30*3
Number of samples	24	24	24	24	24

2.4.1 Molding and curing

In the beginning, a quartz layer with cement (10mm) was put in mechanically vibrated mold with a dimension of 30x30x3cm and then the homogenous mixture was poured in the mold. After the mold is filled with mixture, it is subjected to a hydraulic force of 14N/mm^2. Then, the formed tiles were de-molded and put in humid conditions for two days. For curing purposes, samples were merged in curing tank for three days and then stored in humid conditions until the day of testing.

2.4.2 Laboratory tests

After 28 days of fabrication, terrazzo tiles samples were tested for transverse strength at drying conditions, absorption, and density. The specimen was placed horizontally on the bearers and subjected to loading with constant increase until the specimen fails. Transverse strength was determined for 12 samples of each batch while the absorption ratio was tested for three randomly selected samples of each batch.

2.5 Utilization of volcanic tuff as a pavement material (CBR Test)

2.5.1 Material and Batching

CBR test was conducted according to D1883-07, where 5 kg sample of volcanic tuff were taken, then water was added to the sample and mixed thoroughly. Spacer disc is placed over the base plate at the bottom of the mold and a coarse filter and a paper is placed over the spacer disc. The mold was cleaned and oil was applied, then the sample was filled in the mold to the 1/5 of the total depth. The layer was compacted by giving 56 evenly distributed blows using a hammer of weight 4.89 kg. The top layer of the compacted sample is scratched and again a second layer is filled and the process was repeated. After the third layer addition, the collar was also attached to the mold and the process was continued. After the fifth layer collar was removed and excess materials were struck off, then the base plate was removed and the mold inverted and it was clamped to a base plate. Surcharge weights of 2.5 kg were placed on the top surface of the sample. Three sample of coarse material (at least half the material is retained on sieve No. 200) and three samples of fine materials (materials passing sieve No. 200) were taken.

2.5.2 Laboratory test

Mold containing specimen was placed in position on the testing machine and the penetration plunger was brought in contact with the sample and a load of 4 kg (seating load) was applied so that contact between sample and plunger was established, then dia1 readings are adjusted to zero and load is applied such that penetration rate is 1 ±0.2 mm per minute and load was recorded. The values in N at penetrations of 2.5 and 5.0 mm were recorded and the bearing ratio for each was calculated. The greatest value calculated for penetrations at 2.5 and 5.0 mm recorded as the CBR.

$$CBR=(Px100)/Ps \quad (2)$$

Where, *P*: Measured pressure for sample (N/mm^2). *Ps*: Achieve pressure at equal penetration standard soil (N/mm^2).

2.5.3 Hardness of raw material

This test was conducted to determine the resistance and degradation of aggregates and its resistance to abrasion impact in the Los Angeles Machine according to ASTM C-131. The test is widely used as an indicator of the relative quality or competence of aggregates. A sample of 5 kg of coarse aggregate ware washed and dried at the oven (103 to 105 °C) to substantially constant weight. The sample was placed in the LA abrasion testing machine, and then the machine was rotated at a speed of 30 to 33 rpm

for 500 revolutions. The materials were discharged from the LA abrasion machine and separated on sieve No. 12 (1.70mm). The weight of material coarser than sieve No. 12 was recorded, and oven-dry to a constant mass (105). After cooling, the mass was recorded.

3 Results and Discussion

3.1 Utilization of volcanic tuff in bricks formulation

After 24 hours, the formed bricks were removed from the molds, and it was found that the samples number B_4 and B_5 were not formed and no cohesion occurred as the material threw out after de-molding. Samples number B_4 and B_5 with a high ratio of volcanic tuff (75% and 100%) show high water absorption which decreased the available water for reaction and therefore become insufficient to complete the hydration process and subsequently to harden the bricks. Sample number B2 with 25% volcanic ratio provided the highest compression strength equal to 8.7 MPa whereas, B_1 (control) reported 6.44 MPa and finally the lowest value was recorded for B_3 with 5.96 MPa (**Figure 1.a**). Although all batches achieved Jordanian standards for unloaded bricks of 3.44 MPa (70kg/cm^2), only B_2 was complied with Jordanian standards for loaded bricks of 6.87MPa (70kg/cm^2). This result indicated that low substation of normal aggregate with volcanic tuff (25%) can be used successfully to improve the compressive strength of bricks. This result is in line with that obtained by Al-Zboon and Al-Zou'by (2017), they reported that the substitution of VT with 25% improved the compression strength of concrete. Also, Al Dwairi *et al*., 2018 reported that VT improved the strength characteristics of concrete. The dry weight of bricks' samples decreased from 12.8 kg/brick for B_1 to12.6 and to 11.73 kg/brick for B_2 and B_3, respectively, showing an increase in density by 2% and 8.6%, respectively (**Figure 1.b**). This reduction is probably due to the lower density of volcanic tuff in comparison with normal aggregates. In contrast, the absorption ratio increased significantly with VT increase (Figure 1 c). Higher absorption of B_2 and B_3 is attributed to the higher water absorption of the raw material (VT) due to the high voids ratio and specific surface area. Many researchers found that the adding of VT to the concrete and cement mortar mixture increased water absorption and reduced density (Al-Zboon, and Al-Zou'by, 2014; 2017).

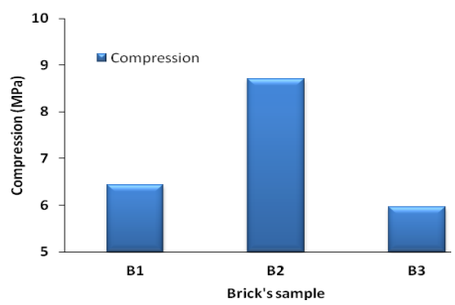

Fig. 1.a Compression strength of bricks

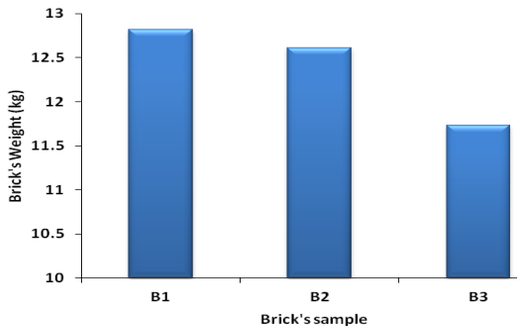

Fig. 1.b Bricks dry weight test.

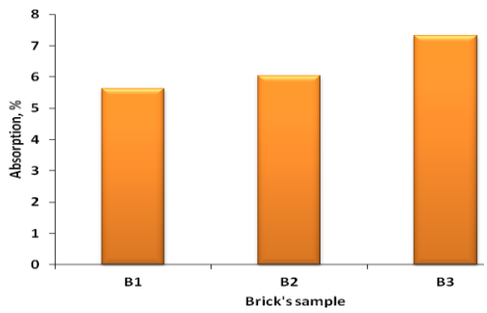

Fig. 1.c Bricks water absorption

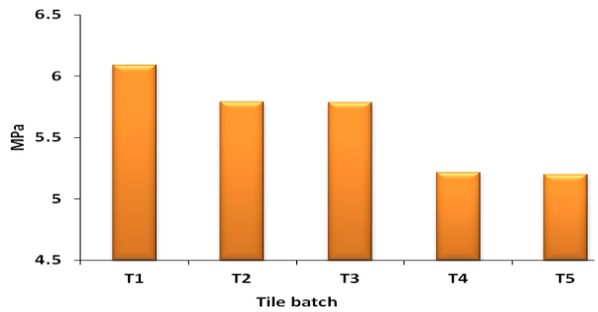

Fig. 2.a Terazzo tiles tranverse strength

3.2 Utilization of volcanic tuff in terrazzo tiles formulation

After 28 hours, the formed tiles were tested for transverse strength. The obtained results indicated that the average transverse strength of all tested batches exceeded the value limited in Jordanian standards (30 kg/cm^{-2}, 2.94MPa). The strength values of the tested samples range from 5.21-6.08 MPa in comparison with the control batch (T1), transverse strength of tiles decreased by 4.91, 4.97, 14.3, and 14.6% for T_2, T_3, T_4, and T_5, respectively (**Figure 2.a**). While T_2 and T_3 showed a slight decrease in the transverse strength, T3 and T4 showed a high reduction. Good strength of VT may be attributed to the high content of SiO_2 which plays a significant role in the strength especially at the early age of the construction material (Ababneh and Matalkah, 2018). The fine silica in VT can combine with calcium hydroxide to form stable compounds like calcium silicates, which have cementation properties (Al Dwairi *et al*., 2018). These results revealed that the use of VT with a mixture up to 50% ratio (T_3), did

not affect the strength significantly. These results indicate that the volcanic aggregates could be used, with a high percentage, in the bottom layer of terrazzo tiles. Regarding the density, it was found that there is no significant difference between all samples, where the weight of a tile ranged from 7.32 for T_1, to 6.93 kg for T_5 with a 5.2% reduction (**Figure 2.b**). Lower density of produced tiles was attributed to the lower density of VT in comparison with NA as mentioned above. Kavasa and Evcin (2005) found that VT can be used successfully in the production of wall tiles with an insignificant impact on the compressive strength at replacement ratio of 9, 14, 15%wt. Abu baker (2009) found that the utilization of volcanic tuff in concrete mixture resulted in a reduction in concrete density by 14%. Absorption ration increased from 1.1 for T_1 to 2.0, 2.6, 4.6, and 5.3 for T_2, T_3, T_4, and T_5, respectively (**Figure 2.c**). Due to its high voids and surface area, VT has high water absorption which explains the obtained results. The higher water absorption at higher replacement ratio was attributed to the presence of K_2O (Kavasa and Evcin, 2005).

3.3 Utilization of volcanic tuff as pavement materials (CBR test):

Figure 3 illustrates the results of CBR test. Based on calculation, CBR for the fine and coarse materials were 28.8% and 33.33%, respectively. Therefore, the values of CBR indicate that the materials are considered a good subsidiary for foundation and sub-foundation utilization purposes (**Table 3**).

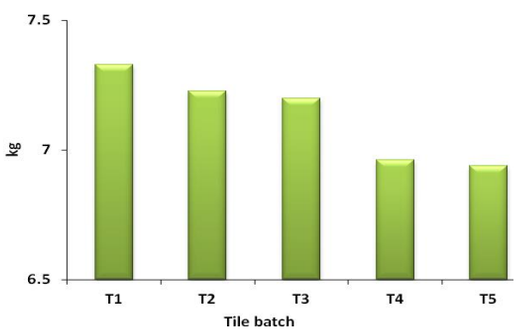

Fig. 2.b Terazzo tiles weight

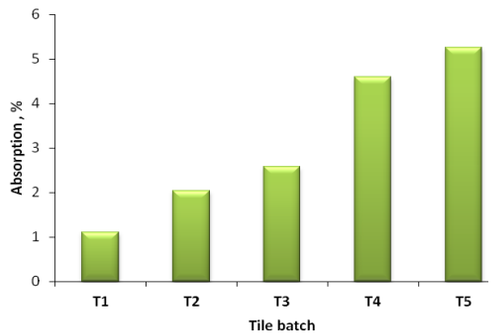

Fig. 2.c Terazzo tiles absorption

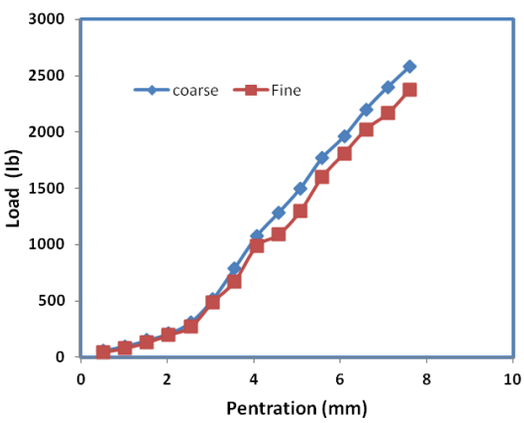

Fig. 3 Result of CBR test.

Table 3 Values of loads and its classifications for different uses.

Loading percent	Materials Classification	Field use
0-3	Very weak	Soil base
3-7	Weak	Soil base
7-2	Acceptable	Under foundation
20-50	Good	Foundation and under foundation
>50	Excellent	Foundation

The calculated Los Angeles Abrasion loss was 27.89%. There is no standard Los Angeles abrasion specification for super pavement mix design. Specifications are typically established by local agencies. Typically, U.S. specifications limit the abrasion of coarse aggregate for hot mix asphalt used to a maximum ranging from 25 to 55%, with most states using a specification of 40 or 45%. Requirements for stone matrix asphalt tend to be lower; AASHTO specifies a maximum Los Angeles abrasion loss of 30% for stone matrix asphalt. The obtained result of the LA test indicated that VT complies with international standards and is suitable to be sued in hot asphalt mixes.

Conclusions

Volcanic tuff is considered an attractive and promising option to be used in various construction projects. The study indicated that bricks sample number B_2 with 25% volcanic ratio provided the highest compression strength equal to 8.7 MPa in comparison with B_1 and B_3 as the lowest value was recorded for B_3 (75%) as 5.96 MPa. Moreover, the dry weight of the sample decreased from 12.8 kg/brick for B_1 to 11.73 kg/brick for B_3, provided lower density construction material. However, the absorption ratio of

samples increased from for B_1 to B_3 representing 5.63% and 7.33% respectively indicating the high water absorption of volcanic tuff. The strength values for all tested samples range from 5.19-6.08.0 MPa and all batches exceeded the limit of JS (2.94 MPa). These results indicate that the use of volcanic aggregate with mixture up to 50% ratio (T_3), did not affect the Terrazzo tiles strength significantly. The density of tiles decreased with VT ratio increase while the absorption ratio increased accordingly. CBR test results for the fine and coarse materials were 28.8% and 33.33%, respectively. Therefore, the values of CBR indicate that the materials are considered as good pavement materials in foundation and sub-foundation purposes. LA Abrasion loss was determined as 27.89% which falls within the specifications limit of coarse aggregate for hot mix asphalt. This research has the following limitations:

1. Samples of terrazzo tiles should be tested for thermal conductivity.
2. Sieve analyses should be done for the test of using VT as a pavement material.
3. It is necessary to conduct a national project for the utilization of VT in concrete applications.

Nomenclature

CBR	=California Bearing Ratio	[-]
MPa	=Mega Pascal	[-]
VT	=Volcanic tuff	[-]
JVT	=Jordan Volcanic tuff	[-]
NA	=Normal Aggregates	[-]
LA	=Los Angeles	[-]
P	=Measured pressure for sample	[N/mm^2]
Ps	=Achieve pressure at equal penetration standard soil	[N/mm^2]
F	=Compressive strength	[kN/cm^2]

References

Ababneh, A., and Matalkah, F."Potential use of Jordanian volcanic tuffs as supplementary cementitious materials", *Case Studies in Const. Mat.*, **8**, 193-202 (2018).

Abali, Y., Bayca, S., and Targan, S. "Evaluation of blends tincal waste, volcanic tuff, bentonite and fly ash for use as a cement admixture", *J. Haz. Mater.*, **131**, 126-130 (2006).

Abu Baker, M. "Comparison of compression strength of light-weight concrete made of volcanic tuff with normal concrete" In *2nd International Engineering Conference*, (2009) Aden, Yemen.

Al Dwairi R., Al Saqarat, B., Shaqour, F., and Sarireh, M. "Characterization of Jordanian Volcanic Tuff and its Potential Use as Lightweight Aggregate", *Jordan J. of Earth and Env. Sci.*, **9**, 127-133 (2018).

Al-Zboon, K., and Al-Zou'by J. "Natural volcanic tuff for sustainable concrete industry", *Jordan J. of Civil Eng.*, **11**, 408-423 (2017).

Al-Zboon, K., and Al-Zou'by J. "Effect of volcanic tuff on the characteristics of cement mortar", *Cerâmica*,**60,** 279-284 (2014)

Balog A., Nicoleta C., Claudiu A.,, and Iluţiu-Varvara, D. "Valorification of volcanic tuff in constructions and materials manufacturing industry" In T*he 7th International Conference Interdisciplinary in Engineering; Petru Maior University of Tirgu Mures*, 10-11 October 2013; Romania, 12 (2014) 323-328.

Augenti, N., and Parisi, F."Constitutive models for tuff masonry under uniaxial compression", *J. Mater. Civ. Eng.*, **22**, 1102-1111 (2010).

Bell, F., Engineering Geology, 2nd Edn., Elsevier, USA, (2007).

Faella, G., Manfredi, G., and Realfonzo, R. "Cyclic behavior of tuff masonry walls under horizontal loading", In: *Proceedings of 6th Canadian Masonry Symposium*; Canada, 317-328 (1992).

Fredrick, O. "A study into the performance of volcanic tuff as partial replacement of river sand in pre-cast concrete", F16/29021/2009 5th year project report (2014).

Johnson R., and De Graff, J. Principles of Engineering Geology, Wiley, (1988).

Kan, A., and Gul, R. "Properties of volcanic tuff sands as a new material for masonry mortar", *Int. J. of Nat. and Eng. Sci.*, **2**, 69-74 (1996).

Kavasa, T., and Evcin, A. "Use of Afyon region (Turkey) volcanic tuffs in wall tile production", *Ind. Cer.,* **25**, 17-19 (2005).

Kılıc, A., Ati, C., Teymen, A., Karahan, O., and Kamuran, A. "The effects of scoria and pumice aggregates on the strength and unit weight of lightweight concrete", *Sci. Res. Essays,* **4**, 961-965 (2009).

Kılınçarslan, S. "The effect of zeolite amount on the physical and mechanical properties of concrete", *Int. J. Phys. Sci.*, **13**, 3041-3046 (2011).

McLean, A.C., and C. Gribble, Geology for Civil Engineers, 2nd Edn., University of Glasgow, Taylor and Francis (2005).

MEMR, Ministry of Energy and Mineral Resources: Mineral Status and Future Opportunity, Volcanic tuff; (2015.

MPWH , Ministry of Public Works and Housing. Specifications of the architectural and civil works, 1st Edn.. Amman, Jordan (1985).

Negis, F., Zeolite-based composites in energy storage, master dissertation, Izmir, Turkey: Izmir Institute of Technology (1999).

Rahn P., Engineering Geology: An Environmental Approach, 2nd Edn., Prentice Hall (1996).

Smadi, M., and Migdady, E. "Properties of high strength tuff light-weight aggregate concrete", *Cement Concr. Comp.*, **12**, 129-135 (1991).

Turkmenoglu, A., and Tankut, A. "Use of tuffs from central Turkey as admixture in pozzolanic cement assessment of their petro-graphical properties", *Cement Concr. Res.*, **32**, 629-637 (2002).

U.S. Bureau of Reclamation (USBR). Concrete Manual, Part 2: A Manual for the Control of Concrete Construction, 9th Edn. Water Resources Technical Publication, U.S. Department of the Interior, Technical Services Center, USBR, Denver, Colorado. (1992).

Yasin, A., Mohammed, T., Hassan, R., and Eid, I. "Effect of volcanic tuff on concrete compressive strength", *Contemp. Eng. Sci.,* **5**, 295-306 (2012).